

# Full 3D anisotropic estimation of tissue in ultrasound imaging

Emeline TURQUIN<sup>1</sup>, Lorena PETRUSCA<sup>1</sup>, Magalie VIALON<sup>1,2</sup>, Hervé LIEBGOTT<sup>1</sup>  
and François VARRAY<sup>1</sup>

<sup>1</sup>Univ Lyon, INSA-Lyon, Université Claude Bernard Lyon 1, UJM-Saint Etienne, CNRS, Inserm, CREATIS UMR 5220, U1206, F-69621, LYON, France

<sup>2</sup>Radiology Dept. CHU de Saint-Etienne, Univ Lyon, UJM Saint-Etienne, F-42023, SAINT-ETIENNE, France

**Abstract**— In cardiac diseases or after myocardial infarction, the fibrous layout in the heart can be modified. To determine the local fiber orientation and to characterize the lesion, an imaging method is required. The fiber orientation can be determined by diffusion MRI, but various factors limit its use in a beating heart. It has been demonstrated that ultrafast ultrasound imaging can measure the local fiber orientation of an *in vivo* heart based on the ultrasound spatial coherence. This method only returns the fiber orientations in planes parallel to the probe surface. We propose a method called 3D coherence function to improve this initial strategy to extract the full 3D local anisotropy. To validate this approach, 3D ultrasound datasets were acquired on a phantom constituted of several wire layers mimicking different fiber layers. The acquisitions were conducted with different angles between the probe surface and the wire layers. For each dataset, the conventional approach and our 3D coherence function were computed to compare the improvement in the fiber angle evaluation. We have demonstrated that when the out-of-plane angle increases, the 3D coherence function allows a better extraction of the angle.

**Keywords**— *ultrasound, heart, fibers, spatial coherence, 3D.*

## I. INTRODUCTION

The microstructure of the heart muscle is very complex. The myocardial tissue is composed by muscular fibers whose orientation changes as a function of their spatial location on the heart and their depth inside the tissue. This layout allows the heart to contract in many directions and to eject the blood in the aorta to supply the organs with oxygen, nutrients, etc.

Due to various pathologies, this fibrous layout can be modified. For example, during a myocardial infarction, a coronary artery is blocked and cells are no more supplied with blood. A lesion will appear due to this cells death. The consequence is the rearrangement of the cardiac tissue inside the lesion [1].

A method able to render the local orientation of the fibers can be useful to determine the modification of orientation and to characterize the lesion. In this field, diffusion MRI is the reference [2]. Because of its long acquisition time (approximately 20 minutes), MRI is not the most suited modality to image a moving object as the heart. Recent sequencing strategies have greatly accelerated the acquisition time but are still limited for imaging an entire *in vivo* beating heart. On the contrary, ultrasound imaging can acquire data

faster than several thousand images per second and appears to be the best imaging candidate for cardiac applications.

In the literature, three methods have been described for extracting the fibers orientation using ultrasound imaging: the backscatter coefficient [3], the shear wave velocity [4] and the spatial coherence [5]. Because it appears as the most promising approach, we have chosen to base our work on the spatial coherence method. It was first developed for focused transmission for Non Destructive Evaluation (NDE) of composite materials [6]. Then, it was extended to medical imaging by Papadacci *et al.* with plane wave transmissions and on 3D data [5]. However, this method can only extract the fiber orientation in a plane parallel to the probe surface. The objective of this work was to extend this method so as to extract the full 3D orientation that is to say the angle in the plane parallel to the probe but also the out-of-plane angle.

## II. METHOD

Initially, the spatial coherence was developed by Arnaud Derode and Mathias Fink with focused waves. They showed that the coherence of the backscatter field is directly linked to the organization or structure of the insonified tissue at the focal point [6]. The tissue organization can then be determined at different locations by simply analyzing the backscattered field received after a focused transmission in those different locations. They showed that if the tissue is isotropic, the backscattered field is incoherent whereas if it is anisotropic, the backscatter field will be coherent in its principal direction [6]. Computing the coherence function necessitates focalized signals. Focusing signals on each point of the tissue would be too long especially for cardiac applications.

Since it is possible to create a synthetic focalization with much less transmissions, plane wave strategies were investigated as a solution to extend the coherence function for cardiac imaging [5, 7]. To create the focalization in any spatial position in reception, it is necessary to calculate the time-of-flight for the wave to travel from the computed point to all the elements of the probe. Then, to create the synthetic focalization in emission, one needs simply to sum up coherently such focused received signals from different steered plane waves [8]. Since the field is now focused at any position in the medium, the coherence function can be computed anywhere.

### A. The 2D spatial coherence

The 2D coherence function is based on the correlation of the focalized signals. The single elements signals are correlated pairwise as a function of their distance in  $x$  and  $y$  direction. This function can be expressed as [5]:

$$R(\Delta x, \Delta y) = \frac{1}{N_x - |\Delta x|} \frac{1}{N_y - |\Delta y|} \sum_i \sum_j \frac{\sum_{t=T_1}^{T_2} S(i, j, t) S(i + \Delta x, j + \Delta y, t)}{\sqrt{\sum_{t=T_1}^{T_2} S(i, j, t)^2 \cdot \sum_{t=T_1}^{T_2} S(i + \Delta x, j + \Delta y, t)^2}} \quad (1)$$

where  $S(i, j, t)$  are the focalized signals received by the element  $(i, j)$  in the  $(x, y)$  direction,  $[T_1; T_2]$  is the temporal window,  $N_x$  and  $N_y$  are the numbers of correlated signals in the  $x$  and  $y$  directions,  $\Delta x$  and  $\Delta y$  are the distances between two correlated signals in the  $x$  and  $y$  directions.

If the medium is isotropic, the signals will be different in all directions. So the coherence map will be a circle or a diamond (Figure 1 (a)). On the contrary, if the medium is anisotropic (it has a main orientation), the signals will be coherent in a given direction and the coherence map will exhibit an ellipse (Figure 1 (b)). So, by analysing the shape of the coherence map, the local orientation of tissue can be extracted.

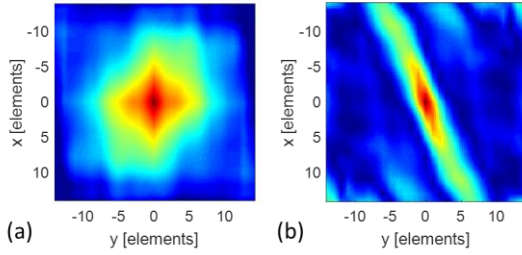


Figure 1 – Examples of 2D coherence maps for (a) an isotropic and (b) an anisotropic medium.

### B. The 3D spatial coherence

As for the 2D coherence function, the 3D coherence function is based on the correlation of the focalized signals in function of their distance. In this new approach, the correlation is computed in  $x$  and  $y$  direction as previously, but also in  $z$  direction. It allows extracting the out-of-plane angle located in the focalized signals ( $\varphi$  angle). The 3D coherence function can be expressed as:

$$R(\Delta x, \Delta y, \Delta z) = \frac{1}{N_x - |\Delta x|} \frac{1}{N_y - |\Delta y|} \sum_i \sum_j \frac{\sum_{t=T_1}^{T_2} S(i, j, t) S(i + \Delta x, j + \Delta y, t + \Delta z)}{\sqrt{\sum_{t=T_1}^{T_2} S(i, j, t)^2 \cdot \sum_{t=T_1}^{T_2} S(i + \Delta x, j + \Delta y, t + \Delta z)^2}} \quad (2)$$

where  $S(i, j, t)$  are the focalized signal received by the element  $(i, j)$  in the directions  $(x, y)$ ,  $[T_1; T_2]$  is the temporal window,  $N_x$  and  $N_y$  are the numbers of correlated signals in the  $x$  and  $y$  directions,  $\Delta x$ ,  $\Delta y$  and  $\Delta z$  are the distances between two correlated signals in the  $x$ ,  $y$  and  $z$  directions.

The shape of the 3D coherence function (3DCF) depends on the medium. If the medium is isotropic, the 3DCF will be a sphere. On the contrary, if the medium is anisotropic, the 3DCF will exhibit an ellipsoidal shape in the principal direction. This ellipsoid can be defined by two angles. The first one is called  $\theta$ . It is the angle in the plane  $xy$  (the same as for the 2DCF). The second one is called  $\varphi$  and is the out-of-plane angle. A schematic representation on these angles is proposed on Figure 2.

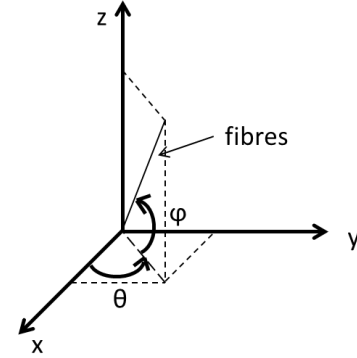


Figure 2 – Representation of the definition of the different angles in 3D.

### C. The fractional anisotropy

In an anisotropic medium, the 2D coherence function exhibits an ellipse shape. In order to quantify how much the local tissue is anisotropic, the ratio between the short and the long axis of the ellipse can be used. The higher the ratio, the stronger the anisotropy is. In order to quantify the anisotropy, the fractional anisotropy can be used and it is expressed as [5]:

$$FA = \sqrt{2} \frac{\left( PA - \frac{GA + PA}{2} \right)^2 + \left( GA - \frac{GA + PA}{2} \right)^2}{PA^2 + GA^2} \quad (3)$$

where PA and GA are the length of the short and long axis of the ellipse.

This anisotropy is normalized between zero and one, and can be expressed in percentage.

The 3D coherence function exhibits an ellipsoidal shape in the case of an anisotropic tissue. This ellipsoid can have a principal axis very long compared to the middle and the small axes, or the principal axis can be very close to the middle axis. What is important to characterize the anisotropy is the difference between the principal axis and the middle axis in order to have only one principal direction. So we propose to use the equation (3) with the middle axis instead of the small axis.

The fractional anisotropy (FA) is used in order to remove points for which the FA value is below a certain threshold that is to say the coherence function is almost a circle or a sphere. In the following, a threshold of 30% is defined. This means that values with a FA less than 30% are not considered.

#### D. Experimental set-up

The experimental set-up is composed by four Verasonics Vantages 256 systems (Verasonics Inc., USA) synchronized together. A  $32 \times 32$  matrix ultrasound probe is connected to the system to controlled the 1024 elements in both transmit and receive [9] (Figure 3 (a)). The central frequency of the probe is 3 MHz and the sampling frequency is 12 MHz. The pitch in  $x$  and  $y$  direction is  $300 \mu\text{m}$ .

Data were acquired on a home-made phantom (Figure 3 (b)). It is a disk with a  $40 \times 45 \text{ mm}$  window. A wire has been wound approximately in the same direction in order to create four layers on the entire window. This handmade phantom creates variability between the different wires. The phantom thickness is approximately 3 mm, while the diameter of the wire is  $100 \mu\text{m}$ .

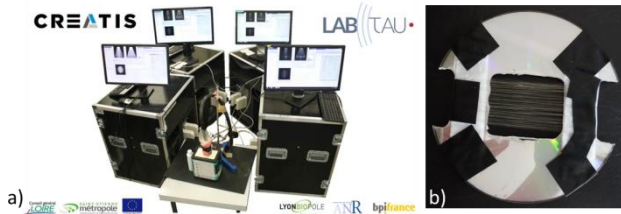


Figure 3 – Picture of (a) the experimental set-up with four Verasonics US systems and a matrix probe and (b) the disk phantom.

In order to acquire data on the disk with different  $\varphi$  angles, a manual rotating platform was used. It was fixed on a plate arranged to a wall of a tub where the acquisitions are made. Then a 3D printed piece was fixed to the rotating platform (Figure 4) to add different  $\varphi$  angle in the direction of the wire to respect the Figure 2.

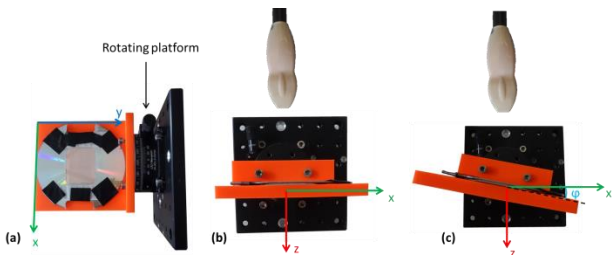


Figure 4 – Pictures of the experimental set-up including the US probe and the rotating platform used to add different  $\varphi$  angles on the phantom, (a) top view, (b-c) front view without and with out-of-plane angle.

Before starting the acquisitions, the surface of the probe was aligned with the printed piece to be sure that the first dataset was without  $\varphi$  angle.

Data were acquired with plane wave transmissions. Nine waves from  $-10^\circ$  to  $10^\circ$  were sent in both  $x$  and  $y$  directions for 81 transmissions in total.

### III. RESULTS

Data were acquired for  $\theta = 0^\circ, 45^\circ$  and  $90^\circ$  and for  $\varphi = 0^\circ, 3^\circ, 6^\circ, 9^\circ$  and  $12^\circ$ . It conducted to 15 different datasets. For each dataset, the 2D coherence function and the 3D coherence function were computed on each point in front of each probe element in  $x$  and  $y$  direction and with a step of  $0.1 \text{ mm}$  in  $z$  direction on a depth from  $52 \text{ mm}$  to  $63 \text{ mm}$ . For both methods, the  $\theta$  angle was extracted. The histogram of the angle representing the angle dispersion is plotted on Figure 5 for each dataset and with both methods.

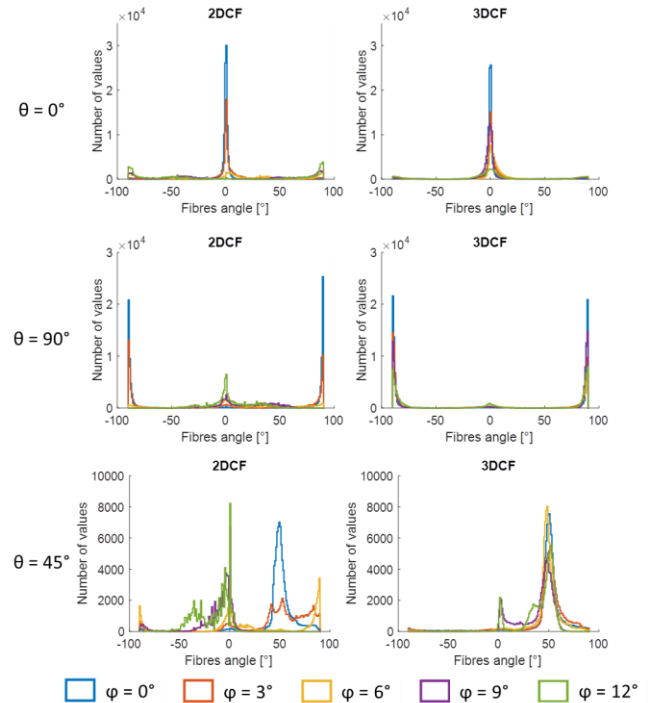


Figure 5 – Histograms of the  $\theta$  angle extracted with the 2D coherence function and the 3D coherence function for different  $\theta$  ( $0^\circ, 90^\circ$  and  $45^\circ$ ) and for  $\varphi = 0^\circ, 3^\circ, 6^\circ, 9^\circ$  and  $12^\circ$ .

The histograms show that when the out-of-plane angle  $\varphi$  increases, the 2DCF does not extract the good  $\theta$  angle whereas the 3DCF is still able to extract it properly. For example, for the dataset with  $\theta = 45^\circ$ , when  $\varphi$  is superior to  $3^\circ$ , the  $\theta$  angle extracted with 2DCF is  $0^\circ$  whereas with the 3DCF the angle extracted is all the time the good one. This observation is the same for  $\theta = 90^\circ$ . For the dataset with  $\theta = 0^\circ$ ,  $\varphi = 12^\circ$ , and with the 2DCF, there are more values at  $90^\circ$  than at  $0^\circ$ . On the contrary, with the 3DCF, when  $\varphi$  increases the number of values having estimated properly decreases (due to FA which is lower), but the values extracted are still correct.

The results can also be represented by tractography. It consists in representing the orientation of a medium by curves respecting as much as possible the angle obtained at each point. It is often used in MRI to represent the fibers in the brain or in

the heart. An example is plotted on the Figure 6 for the dataset with  $\theta = 45^\circ$  and  $\varphi = 6^\circ$ . The tractography obtained with the 2DCF (Figure 6 (a)) has two different orientations (two colors) at  $0^\circ$  and  $90^\circ$  whereas with the 3DCF (Figure 6 (b)), there is mainly one orientation (one color). This confirms the previous observations.

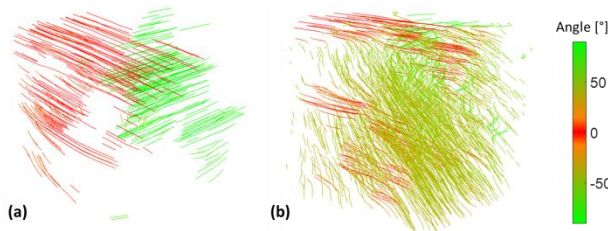


Figure 6 – Tractographies of the dataset with  $\theta = 45^\circ$  and  $\varphi = 6^\circ$  obtained with (a) the 2D coherence function and (b) the 3D coherence function.

#### IV. DISCUSSION AND CONCLUSION

The coherence method presented in the literature to extract cardiac structure imaging allows only extracting the angle in the plane parallel to the probe surface ( $\theta$  angle). We have proposed to correlate the signals in  $x$ ,  $y$  but also in  $z$  direction in order to extract the full 3D orientation: the  $\theta$  angle but also the out-of-plane angle. The method was validated on datasets acquired on a phantom constituted by wire layers. The 2DCF and 3DCF were computed on all datasets for comparison purposes.

The extraction of the  $\theta$  angle is better with the 3DCF than with the 2DCF especially when the  $\varphi$  angle increases. Moreover, the 3DCF allows also extracting the  $\varphi$  angle. When this angle increases in the medium, the angle extracted increases too but the quantitative values are not the right ones. The theory has to be further investigated to identify the link between the  $\varphi$  angle extracted and the  $\varphi$  angle present in the medium.

We could study the impact of the angle of plane waves. However, it depends of the study depth. If the medium is too deep, the medium could not be insonified by a high tilted angle. Here, the phantom was positioned between 52 and 63 mm depth. So the maximum angle of  $10^\circ$  seems to be the best compromise.

Next, these results have to be confirmed on *in vivo* data on a skeletal muscle first because the fiber is almost in the same direction. Then, data have to be acquired on an *ex vivo* heart which is a more complex tissue and it is difficult to put the probe parallel to the fiber.

In conclusion, our proposed 3D coherence function allows to better extract the  $\theta$  angle compared to the 2DCF when out-of-plane orientation is present. Moreover, the out-of-plane measure need to be further studied to extract the full 3D orientation.

#### ACKNOWLEDGMENT

This work was supported by the LABEX PRIMES (ANR-11-LABX-0063) of Université de Lyon, within the program "Investissements d'Avenir" (ANR-11-IDEX-0007) operated by the French National Research Agency (ANR). The RF Verasonics generator was cofounded by the FEDER program, Saint-Etienne Metropole (SME) and Conseil General de la Loire (CG42) within the framework of the SonoCardio-Protection Project led by Pr Pierre Croisille. The authors would like to thank LabTAU for their contribution in the development of the 32x32 probe prototype compatible with a driving by 1 to 4 Verasonics Vantage 256 as well as for the provision of the probe and two Vantage 256 systems.

#### REFERENCES

- [1] J. Cleutjens, W. Blankesteyn, M. Daemen et J. Smits, « The infarcted myocardium : Simply dead tissue, or a lively target for therapeutic interventions », *Cardiovascular Research*, vol. 44, n°2, p. 232-241.
- [2] H. Lombaert, J-M Peyrat, P. Croisille, S. Rapacch, L. Fanton, C. Farida, P. Clarysse, I. Magnin, H. Delingette and N. Ayache, "Human Atlas of the Cardiac Fiber Architecture: Study on a Healthy Population", *IEEE Transactions on medical imaging*, vol. 31, n°7, p. 1436-1447, 2012.
- [3] M. Milne, G. Singh, J. Miller et M. Holland, « Echocardiographic-Based Assessment of Myocardial Fiber Structure in Individual, Excised Hearts », *Ultrasonics Imaging*, vol. 34, n°3, p. 129-141, 2012.
- [4] W.-N. Lee, M. Pernot, M. Couade, E. Messas, P. Bruneval, A. Bel, A. A. Hagège, M. Fink et M. Tanter, "Mapping Myocardial Fiber Orientation Using Echocardiography-Based Shear Wave Imaging", *IEEE Transactions on medical imaging*, vol. 31, n°3, p. 554-562, 2012.
- [5] C. Papadacci, V. Finel, J. Provost, O. Villemain, P. Bruneval, J-L Gennisson, M. Tanter, M. Fink and M. Pernot, « Imaging the dynamics of cardiac fiber orientation in vivo using 3D ultrasound Backscatter Tensor Imaging », *Nature Scientific Reports*, 2017.
- [6] M. Fink and A. Derode, "Spatial Coherence of Ultrasonic Speckle in composites", *IEEE Transactions on ultrasonics, ferroelectrics, and frequency control*, vol. 40, n°6, p. 666-675, 1993.
- [7] C. Papadacci, "Imagerie échographique ultrarapide du coeur et des artères chez l'homme : Vers l'imagerie ultrarapide 3D et l'imagerie du tenseur de rétrodiffusion ultrasonore », *Medical Physics*, Université Paris-Diderot, Paris 7, 2014.
- [8] G. Montaldo, M. Tanter, J. Bercoff, N. Benech and M. Fink, "Coherent Plane-Wave Compounding for Very High Frame Rate Ultrasonography and Transient", *IEEE Transactions on ultrasonics, ferroelectrics, and frequency control*, vol. 56, n°3, p. 489-506, 2009.
- [9] L. Petrusca, F. Varray, R. Souchon, A. Bernard, J-Y. Chapelon, H. Liebgott, W.A. N'Djin and M. Viallon, "Fast Volumetric Ultrasound B-Mode and Doppler Imaging with a New High-Channels Density Platform for Advanced 4D Cardiac Imaging/Therapy", *Applied Sciences*, vol. 8, n°2, p200, 2018.